Desalination and Water Treatment
www.deswater.com
doi: 10.1080/19443994.2015.1029527

57 (2016) 8739–8747
April

Taylor & Francis
Taylor & Francis Group

Preparation of iron oxide-loaded bamboo charcoals and their trinitrotoluene red water treatment

Hongtao Ran[a,*], Penggang Li[b], Henan Li[b], Chengwan Wu[b], Yihe Zhang[b,*], Yong Ma[b]

[a]*College of Science, Beijing Forestry University, No. 35, Qinghua East Road, Haidian District, Beijing 100083, China, Tel. +86 10 62336188; email: xiaoran@bjfu.edu.cn*
[b]*National Laboratory of Mineral Materials, School of Materials Science and Technology, China University of Geosciences, No. 29, Xueyuan Road, Haidian District, Beijing 100083, China, Tel. +86 10 82322759; emails: 809639086@qq.com (P. Li), 816942076@qq.com (H. Li), 354841026@qq.com (C. Wu), Tel. +86 10 82322759; Fax: +86 10 82322345; email: yhz@cugb.edu.cn (Y. Zhang), Tel. +86 10 82322759; email: 907936935@qq.com (Y. Ma)*

Received 17 July 2014; Accepted 28 February 2015

ABSTRACT

Magnetic bamboo charcoals were prepared by loading $FeCl_3$ onto bamboo charcoal and then calcinated at appropriate temperatures. The type of iron oxides on bamboo charcoal and the possible reactions in the process of preparation were analyzed by thermal gravimetric analysis, X-ray fluorescence, and X ray diffraction. The sample obtained by calcination at 400˚C was the composite of FeO(OH), α-Fe_2O_3, and bamboo charcoal, while the product given by calcination at 700˚C composed α-Fe_2O_3, Fe_3O_4, and SiO_2. The magnetic bamboo charcoal calcinated at 400˚C had a magnetization of 1.12 emu/g and a slightly higher chemical oxygen demand removal rate to trinitrotoluene red water compared to bamboo charcoal. So, the as-prepared magnetic bamboo charcoals were a kind of useful adsorbents with magnetic separation function.

Keywords: Bamboo charcoals; TNT red water; Iron oxide; Magnetization

1. Introduction

Porous materials are widely used as industrial adsorbents because of their high surface area, large pore volumes, chemical inertness, good mechanical stability, and good thermal stability. In recent years, there are growing interests in new applications of porous carbons because of their ability to interact with molecules not only at their out surfaces but also in the interior pores [1–3]. Among these porous carbons, bamboo-based carbon adsorbents have great potential due to their low cost and strong adsorption ability for organic pollutants [4–7] and metal ions [8–10]. For example, Ahmad and Hameed [6] used activated carbon prepared from bamboo waste as an adsorbent for the removal of chemical oxygen demand (COD) and color of cotton textile mill wastewater; 93.08% of color and 73.98% of COD removal are reached. Our group [7] applied bamboo charcoal as an adsorbent of organic pollution in trinitrotoluene (TNT) red water. The equilibrium adsorption model and adsorption kinetic model were studied.

Multifunctional material is a useful tool expected to perform several functions concurrently based on its wide classes of properties. Therefore, bamboo charcoal-based catalysts [11,12], anti-micro-organism

*Corresponding authors.

[13,14], and biofilm-supporting carriers [15] are developed. Recently, carbon composites with magnetic separation function have been developed and used as high-efficiency adsorbents for removal of pollutants from aqueous solutions. The introduction of a magnetic composition (such as maghemite, γ-Fe_2O_3) to carbon-based adsorbents by a pyrolysis activation (simultaneous activation and magnetization) or chemical co-precipitation reaction is an efficient method to enable the adsorbents to be efficiently separated with an external magnetic field [16]. Bamboo charcoal-based iron-containing adsorbent (Fe–BC) was developed using bamboo charcoal as a supporting medium for ferric iron. Column adsorption experiment with Fe–BC showed that Cr(VI) could be removed from 0.12 to below 0.05 mg/L within 360 bed volumes at empty bed with a contact time of 2 min [17]. The composites of bamboo charcoal and Fe_3O_4 nanosheets, as a novel solid-phase microextraction fiber coating, were used for the extraction of seven polybrominated diphenyl ethers (PBDEs) in environmental water samples. The descendent method based on solid-phase microextraction is an excellent method for the routine analysis of PBDEs at trace levels in environmental water samples [18]. So, magnetic bamboo charcoals need to be developed and their novel applications found.

In the present work, industrial magnetic bamboo charcoal was magnetized by simply loading $FeCl_3$ on bamboo charcoal and then calcinated at different temperatures. The crystalline type of iron oxides on bamboo charcoal was clarified. The obtained magnetic bamboo charcoal calcinated at 400°C was used to treat TNT red water which contained a large amount of negative organic pollutants and was produced during the purification of crude TNT by sodium sulfate. The COD removal rate of the final composite to TNT red water was even slightly higher than that of bamboo charcoal.

2. Experimental part

2.1. Materials

Bamboo charcoal was supplied by the Chinese Academy of Forestry, Beijing, China. Bamboo charcoal was washed with distilled water to remove impurities, oven dried at 378 K, and kept in a vacuum desiccator for further use. The TNT red water provided by the number 525 ammunition plant (Hubei Province, China) was reddish-brown with high COD [7]. $FeCl_3{\cdot}6H_2O$ and other chemicals as well as reagents were all purchased from Beijing Chemical Reagent Factory. They were of analytical grade and used without further purification.

2.2. Loading of $FeCl_3$ on bamboo charcoal

In 100 ml of water, 1, 2, 4, 6, 8, and 12 g of $FeCl_3{\cdot}6H_2O$ were dissolved to form 0.004, 0.007, 0.009, 0.015, 0.022, and 0.044 M solutions, then 2 g of bamboo charcoal was added separately to form suspensions. The suspensions were stirred at certain temperatures (25, 40, 50, and 60°C) for 4–5 h to reach adsorption equilibration. The solid was filtered and slightly leached by water to remove the unabsorbed $FeCl_3$.

2.3. Preparation of magnetic bamboo charcoals

The bamboo charcoals loaded with $FeCl_3$ at room temperature from 4 g/100 ml of $FeCl_3{\cdot}6H_2O$ solution were calcinated at 320–800°C in air to study the influence of calcination temperature on the crystalline type of iron oxides. The magnetic bamboo charcoals calcinated at 320, 360, 380, 400, 440, 480, 600, 700, and 800°C were assigned as BC($FeCl_3$)-320, BC($FeCl_3$)-360, BC($FeCl_3$)-380, BC($FeCl_3$)-400, BC($FeCl_3$)-440, BC($FeCl_3$)-480, BC($FeCl_3$)-600, BC($FeCl_3$)-700, and BC($FeCl_3$)-800, respectively. For study of the parameters influencing adsorption, bamboo charcoals loaded with different amounts of $FeCl_3$ at different temperatures were calcinated at 400°C.

2.4. COD removal of TNT red water by BC($FeCl_3$)-400

Batch adsorption experiments were conducted using 0.5 g of BC($FeCl_3$)-400 as the adsorbent in a 250 mL flask containing 25 mL of TNT red water (diluted 50, 100, 125, and 500 times). The flasks were agitated at 150 rpm at room temperature for 2 h. The filtrate was used to test the COD value.

2.5. Characterization

XRD patterns of the mesoporous materials were obtained on a Scintag diffractometer using CuKα ($\lambda = 1.5405$ Å) radiation. Field emission scanning electron microscopy (FE-SEM) patterns were acquired from a LEO-1530 FE-SEM operated at 5 kV. The crude magnetic property of the magnetic bamboo charcoals was used to determine the optimum conditions for composites preparation. A magnet slowly approached to certain amounts of magnetic particles in a plastic bag. The distance between the magnet and the sample beginning to move was the crude magnetic property

of the composites. The average of three times of measurement was used. The magnetization, *Ms*, of the composites as a function of the applied magnetic field, H_0, was measured by a PTMS-9T Vibrating Sample Magnetometer at room temperature. Thermal gravimetric analysis (TGA) was performed on Perkin-Elmer TGA 7 with a heating rate of 20℃/min ranging from 25 to 800℃ in air. The X-ray fluorescence (XRF) method is carried out on a Rigaku ZSX Primus-Ⅱspectrometer to determine the composition of the samples. The COD of TNT red water was determined by potassium dichromate oxidation. The HACH test vials containing potassium dichromate oxidant, catalyst, masking reagent, and TNT red water were put into digestion unit (DRB 200, HACH, USA) and kept for 20 min at 423 K. After cooling and cleaning the vials, the COD of TNT red water was tested by a DR 2800 spectrophotometer (HACH, USA) at a wavelength of 620 nm. The COD removal (%) was calculated as follows:

$$\text{COD removal}\,\% = \frac{C_0 - C_e}{C_0} \times 100\% \quad (1)$$

where C_0 and Ce (mg/L) are the COD of initial and equilibrium TNT red water.

3. Results and discussion

3.1. Optimum conditions for magnetic bamboo charcoals preparation

For obtaining the optimum conditions for magnetic bamboo charcoal preparation, the factors seriously influencing the magnetic property of the target composites such as the initial concentration of $FeCl_3$, adsorption, and calcination temperatures are studied in detail in which a longer adsorption time (4–5 h) for reaching equilibrium adsorption is adopted according to our work on adsorption of TNT red water by bamboo charcoal or activated coke [7,19]. The crude magnetic property of the composites is indicated by the distance between the magnet and certain amounts of the composites at which the composites begin to move toward the magnet as the magnet approaching toward the composites. Therefore, a longer distance indicates stronger magnetic properties. Fig. 1(A) shows the magnetic function of the composites with the initial concentration of $FeCl_3$. As the initial concentration of $FeCl_3$ increases from 0.004 to 0.044 mol/L, the distance for certain amounts of magnetic bamboo charcoals beginning to move with magnet increases from 7.3 to 10 mm and then levels off. The results indicate that as the initial concentration of $FeCl_3$ is 0.009 mol/L, the obtained magnetic composite possesses the strongest magnetic property. So the appropriate initial concentration of $FeCl_3$ for the preparation of magnetic bamboo charcoal is 0.009 mol/L. The effect of the adsorption temperature on the magnetic property of magnetic bamboo charcoals is shown in Fig. 1(B). The distance the magnetic bamboo charcoal begins to move toward magnet almost does not change with the adsorption temperature, which shows that the adsorption temperature has a slight influence on the loaded amount of $FeCl_3$. So in a further study the adsorption of bamboo charcoal to $FeCl_3$ is performed at room temperature.

The effect of the calcination temperature on the magnetic properties of the magnetic bamboo charcoals is shown in Fig. 1(C). The distance for magnetic bamboo charcoals calcinated at different temperatures beginning to move with the magnet increases from ~1 to ~10 mm and then decreases to 3.2 mm, followed by increasing again to ~5 mm. That is the magnetic property of magnetic bamboo charcoals calcinated at 400 or 700℃ is comparatively stronger than the other samples. So it is inferred there are crystal transition in the target composites calcinated at different temperatures. In order to deduce the possible reactions for crystal transition, TGA measurement is performed.

Fig. 2 shows the TGA curves and the corresponding heat adsorption of bamboo charcoal and $FeCl_3$ loaded bamboo charcoal. It is clear that the gasification of bamboo charcoal is mainly at 500–600℃ by finally forming CO_2 (Fig. 2(A)). But in the heat adsorption pattern of bamboo charcoal (Fig. 2(B)), a small heat adsorption peak is observed in the range of 400–500℃. So, a small part of bamboo charcoal is oxidized in 400–500℃ (a), while in the heat adsorption curve of $FeCl_3$ loaded bamboo charcoal, an obvious heat adsorption at ~400℃ is observed corresponding to the decomposition of $FeCl_3$. The gasification temperature of bamboo charcoal is lower shifted after loading $FeCl_3$ which may be caused by the oxidation of Cl_2 produced by $FeCl_3$ decomposition. So the calcination temperature of 400℃ is appropriate for iron oxide formation.

3.2. Formation of iron oxides at different calcination temperatures

In order to confirm the type of iron oxides formed at different calcination temperatures, XRD patterns are performed and shown in Fig. 3. In the XRD pattern of bamboo charcoal (Fig. 3(a)), the characteristic peak at $2\theta = 26.64^{o}$ is the crystalline peak of SiO_2 [20]. After

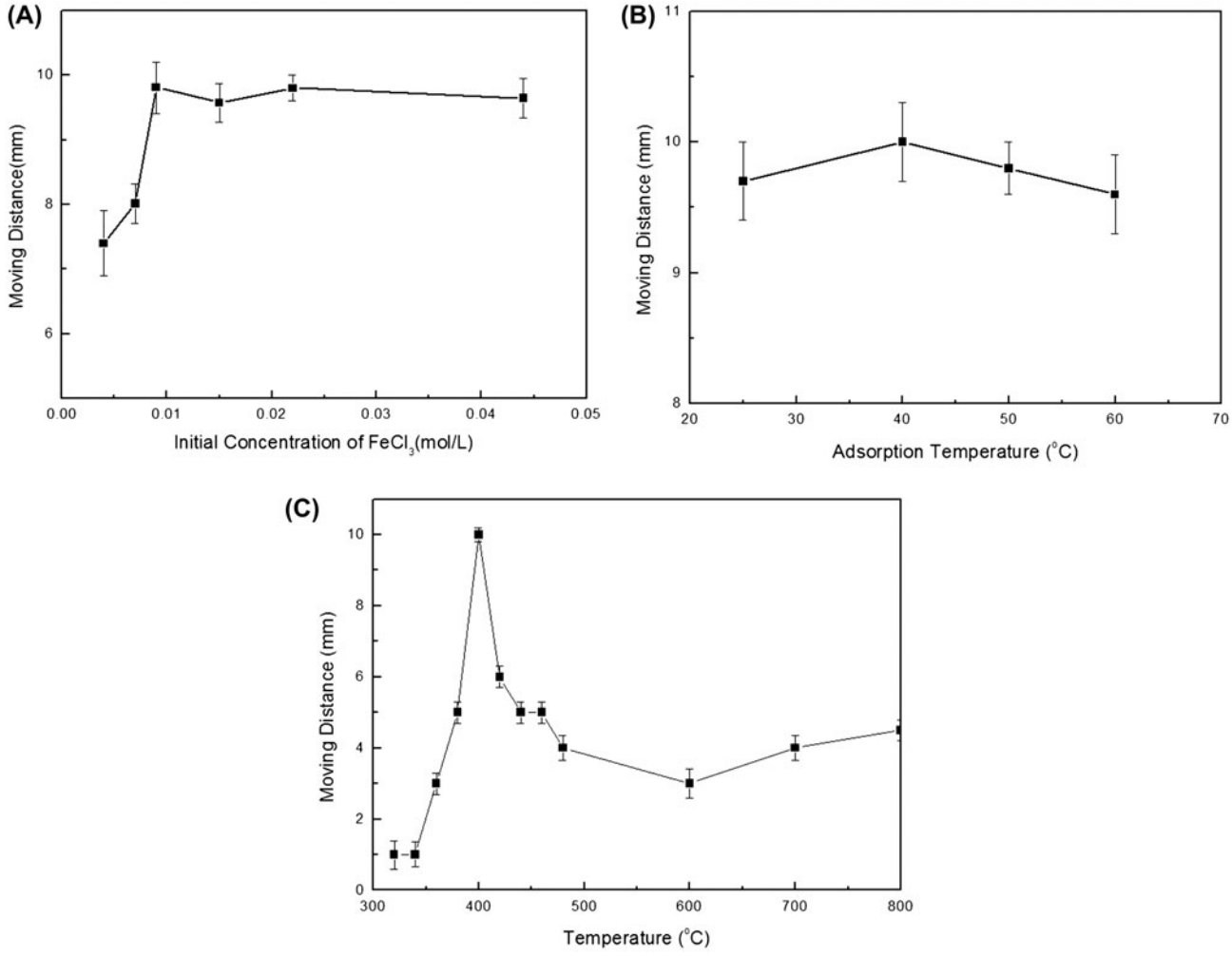

Fig. 1. Effect of the initial concentration of $FeCl_3$ (A), adsorption temperature (B), and calcination temperature (C) on the magnetic property of the magnetic bamboo charcoals.

loading $FeCl_3$, as the calcination temperature is below 400℃, no peak corresponding to iron oxide can be observed (Fig. 3(b) and 3(c)). Further increasing the calcination temperature up to 400℃ (Fig. 3(d)), the diffraction peaks of α-Fe_2O_3 corresponding to (012), (104), (110), (113), (024), and (116) planes become dominant at $2\theta = 24.08$, 35.6, 36.7, 42.48, 49.5′, and 57.56° [21,22]. But diffractions of FeO(OH) at $2\theta = 20.76$ and 36.0046° also can be seen [17], which almost disappear as the calcination temperature is 600℃ (Fig. 3(g)). As the calcination temperature is further increased to 700℃, diffraction peaks of Fe_3O_4 at $2\theta = 30.3$, 36.7, and 54.1° corresponding to (220), (311), and (422) lattice planes (JCPDS 19-0629) are observed [23], meanwhile diffraction peaks of α-Fe_2O_3 become more obvious. Fe_3O_4 being formed at higher tempertures in carbon-based composite is also reported by Bayburtskiy et al. [24].

These XRD results indicate crystalline FeO(OH) and α-Fe_2O_3 are formed together as the temperature is lower than 600℃. At higher calcination temperatures, FeO(OH) disappears and Fe_3O_4 is formed. So it is difficult to form pure magnetic phase, such as FeO(OH), γ-Fe_2O_3, or Fe_3O_4 by calcination of $FeCl_3$ loaded bamboo charcoal. It is reported γ-Fe_2O_3 can only be formed in a narrow temperature range by calcinating the iron precursors. Bulk γ-Fe_2O_3 undergoes a phase transition to α-Fe_2O_3 in a narrow temperature range of 370–600℃ and the phase transition becomes even narrower as γ-Fe_2O_3 is nanometer sized. So strengthening the interaction of iron precursors with the support can widen the phase transition temperature of γ-Fe_2O_3 to α-Fe_2O_3 [25]. In the present work, pure γ-Fe_2O_3 could not been synthesized by calcination indicating that $FeCl_3$

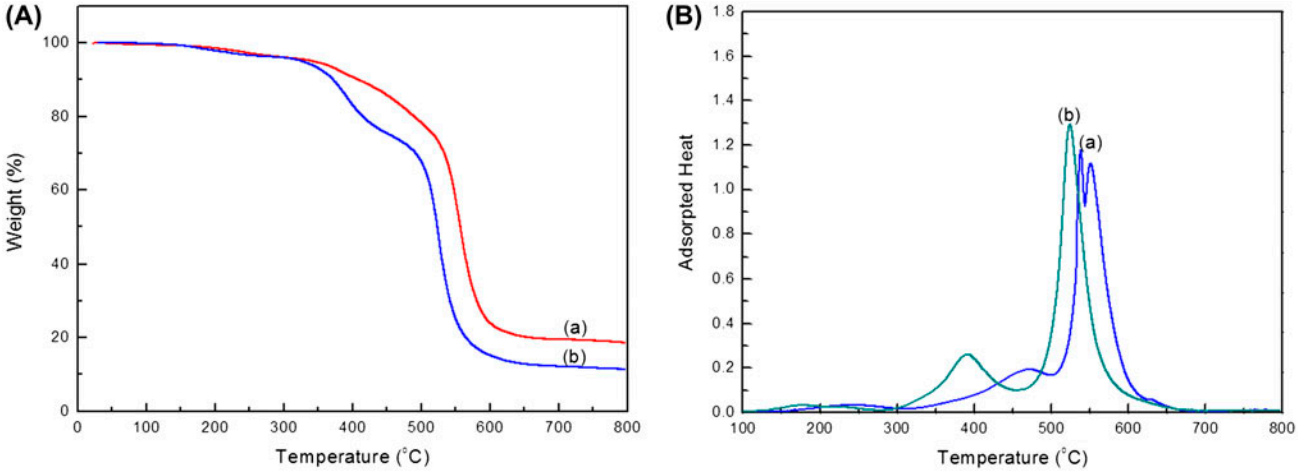

Fig. 2. Weight loss (A) and heat adsorption (B) in the heating process of bamboo charcoal (a) and $FeCl_3$-loaded bamboo charcoal (b).

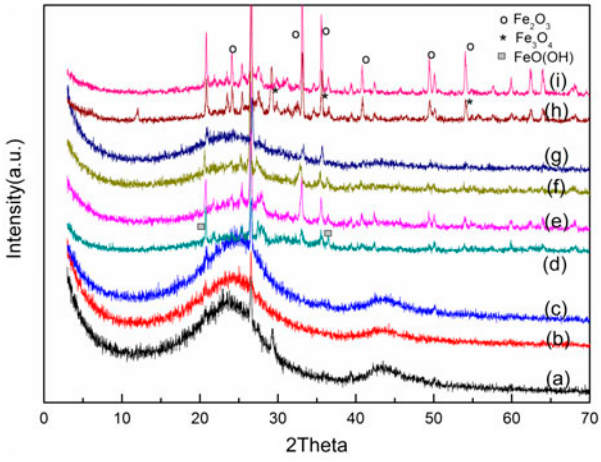

Fig. 3. XRD patterns of bamboo charcoal (a) and magnetic bamboo charcoals formed by calcination at (b) 320, (c) 360, (d) 400, (e) 440, (f) 480, (g) 600, (h) 700, and (i) 800°C.

has poor interaction with bamboo charcoal due to the hydrophilic difference.

Based on the TGA and XRD results it can be inferred that at ~400°C FeO(OH) and α-Fe_2O_3 are formed together by performing reactions (2) and (3).

$$4FeCl_3 + 3O_2 \rightarrow 2\alpha - Fe_2O_3 + 3Cl_2 \quad (2)$$

$$4FeCl_3 + 3O_2 + 2H_2O \rightarrow 4FeO(OH) + 6Cl_2 \quad (3)$$

At a higher calcination temperature (700°C), FeO(OH) could not exist due to its easy decomposition, while the formed α-Fe_2O_3 are partly reduced to Fe_3O_4 due to the reduction of the C gas from bamboo charcoal in the reaction system (formulas (4) and (5)).

$$C(solid) \xrightarrow{\Delta} C(gas) \quad (4)$$

$$6\alpha - Fe_2O_3(s) + C(g) \rightarrow 4Fe_3O_4 + CO_2(g) \quad (5)$$

The disappearance of FeO(OH) and the formation of Fe_3O_4 can well interpret the magnetic property change of the magnetic composites with the calcination temperature shown in Fig. 1(C). This is also the reason why the peak intensity of α-Fe_2O_3 in BC($FeCl_3$)-600, for which the calcination temperature is close to the oxidation temperature of bamboo charcoal (500–600°C, Fig. 2(a)) is lower than that obtained by calcination at 480 and 700°C.

To study the loaded amount of Fe on the bamboo charcoal, XRF was performed. In BC($FeCl_3$)-400, the main elements are C, Fe, and Si and their corresponding mass contents are 68.3, 3.2, and 4.2%. So the loaded Fe is not high enough due to the hydrophobic nature of bamboo charcoal which is friendly to organic matters [4–7].

The morphology of bamboo charcoal and its magnetic composites was studied by electron microscopy and depicted in Fig. 4. It can be seen that bamboo charcoal has a lamellar form with ~2 μm pores vertical to the smooth lamellar surface (Fig. 4(A and B)). But the surface of BC($FeCl_3$)-400 (Fig. 4(C)) becomes crude. In its enlarged photograph (Fig. 4(D)) spherical particles ~50 nm are observed, which can be considered as iron oxide and FeOOH. For BC($FeCl_3$)-700 no matter in low and high magnified photographs obvious

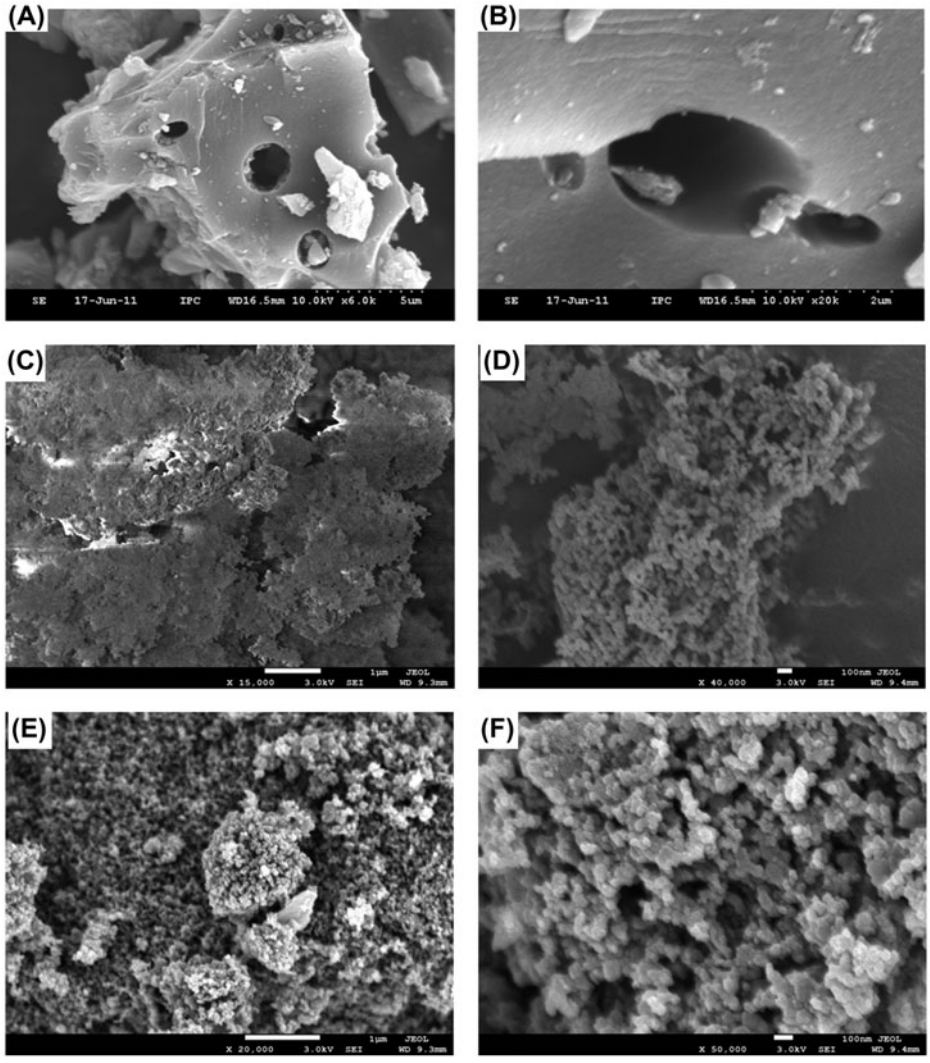

Fig. 4. SEM images of (A,B) bamboo charcoal, (C,D) BC($FeCl_3$)-400, and (E,F) BC($FeCl_3$)-700.

spherical particles with a diameter of 100 nm are obvious. The particle size difference of iron oxides in BC($FeCl_3$)-400 and BC($FeCl_3$)-700 indicates that Fe_3O_4 formed accompany particle amalgamation as the temperature is increased.

3.3. Magnetic properties of the composites

Magnetic measurements were performed to confirm the magnetic nature of the composite particles. Fig. 5(a) and (b) shows M-H curves of the magnetic bamboo charcoal measured at 300 K. The magnetization of BC ($FeCl_3$)-380 and BC($FeCl_3$)-400 reaches saturation and presents a hysteresis loop at the same time, revealing ferromagnetic characteristics of the composites [26], while the magnetization of BC($FeCl_3$)-480 and BC ($FeCl_3$)-700 arises linearly with an increase in the testing magnetic strength. The reason is that the magnetizing current for *Ms* measurement is too high for BC($FeCl_3$)-480 and BC($FeCl_3$)-700 magnetization. In other words, BC($FeCl_3$)-480 and BC($FeCl_3$)-700 are relatively easy magnetization. Among the synthesized samples, BC($FeCl_3$)-400 has the largest *Ms* (1.12 emu/g) and *Hc* (163 Oe). So the calcination temperature of 400˚C for the preparation of magnetic bamboo charcoals is appropriate. Generally, materials with *Hc* higher than 100 Oe are considered as permanent magnetic materials. The higher *Hc* of BC($FeCl_3$)-400 (163 Oe) shows BC($FeCl_3$)-400 has permanent magnetic properties. The *Hc* of BC($FeCl_3$)-380, BC($FeCl_3$)-480˚C, and BC($FeCl_3$)-700˚C is relatively low, which is 45, 32, and 61 Oe, respectively, indicating soft magnetic

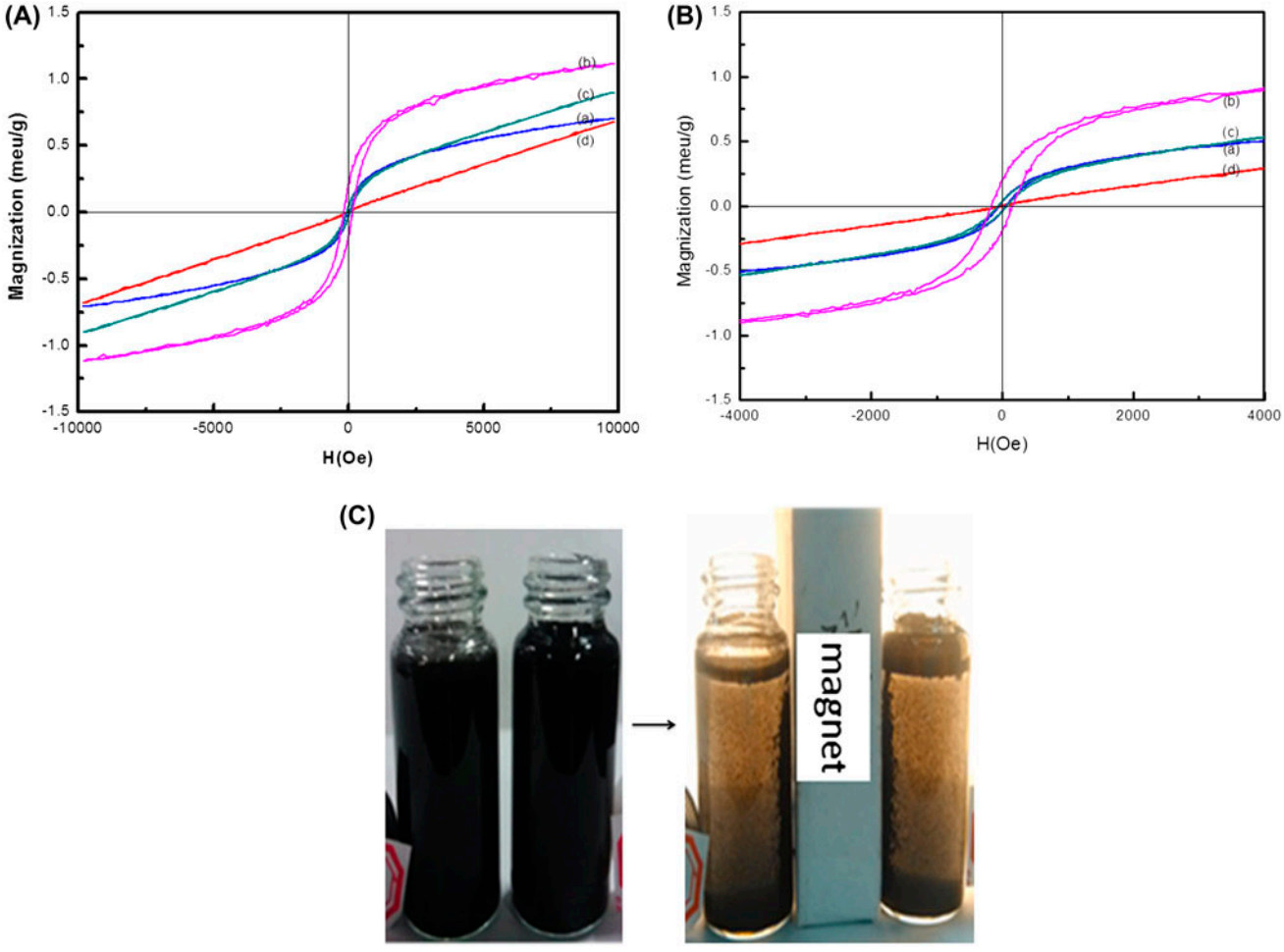

Fig. 5. Magnetization (A,B) of BC($FeCl_3$)-380 (a), BC($FeCl_3$)-400 (b), BC($FeCl_3$)-480℃ (c), and BC($FeCl_3$)-700℃ (d) and the magnetic response of BC($FeCl_3$)-400 (C).

property nature of the composites. The magnetic response ability of BC($FeCl_3$)-400 toward the external magnetic field is shown in Fig. 5(c). As the external magnetic field is 0.6 T, most of BC($FeCl_3$)-400 are adsorbed to the wall of the bottle next to the magnet. That is BC($FeCl_3$)-400 can be magnetically separated from the water as it is used as adsorbent.

3.4. COD removal of BC($FeCl_3$)-400 to TNT red water

As shown in Fig. 6, the removal rate of 0.5 g of bamboo charcoal to 25 mL of TNT red water diluted 50, 100, 125, and 500 times is 34, 60, 67, and 73%, respectively, based on Eq. (1). Under the same conditions, the removal rate of BC($FeCl_3$)-400 to diluted red water is slightly increased which is 37, 63, 69, and 75%. The modified bamboo charcoal still has a higher organic removal rate but possesses magnetic separation function.

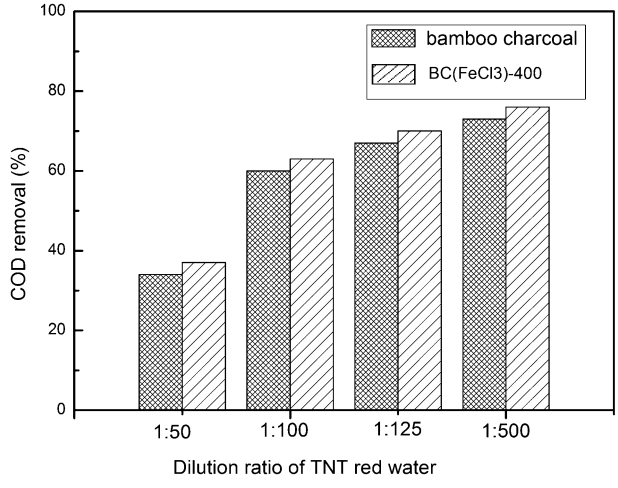

Fig. 6. COD removal rate of bamboo charcoal and BC ($FeCl_3$)-400.

4. Conclusions

Magnetic bamboo charcoals were prepared by loading $FeCl_3$ on bamboo charcoal and then calcinated at appropriate temperatures. The type of iron oxides on bamboo charcoal and the possible reactions were studied through TGA, XRF, and XRD. Also the morphology of the iron oxides was characterized by SEM. BC($FeCl_3$)-400 was the composite of FeO(OH), α-Fe_2O_3, and bamboo charcoal, while BC($FeCl_3$)-700 composed of α-Fe_2O_3, Fe_3O_4, and SiO_2, since the gasification of bamboo charcoal at 700˚C produces SiO_2 residue and reduction gases (C or CO) which reduce part of α-Fe_2O_3 to Fe_3O_4. BC($FeCl_3$)-400 has *Ms* of 1.12 emu/g and a slightly higher COD removal rate to TNT red water compared to bamboo charcoal. So the composite is a useful adsorbent with magnetic separation function.

Acknowledgement

This work is supported by the Fundamental Research Funds for the Central Universities (TD2014-05 and 2-9-2013-49).

References

[1] B. Sakintuna, Y. Yürüm, Templated porous carbons: A review article, Ind. Eng. Chem. Res. 44 (2005) 2893–2902.
[2] Q. Zhou, Z. Li, C. Shuang, A. Li, M. Zhang, M. Wang, Efficient removal of tetracycline by reusable magnetic microspheres with a high surface area, Chem. Eng. J. 210 (2012) 350–356.
[3] P. Hu, Y.H. Zhang, K. Tong, F.F. Wei, Q. An, X.K. Wang, P.K. Chu, F.Z. Lv, Removal of organic pollutants from red water by magnetic-activated coke, Desalin. Water Treat. (2014), doi: 10.1080/19443994.2014.903204.
[4] K. Mizuta, T. Matsumoto, Y. Hatate, K. Nishihara, T. Nakanish, Removal of nitrate-nitrogen from drinking water using bamboo powder charcoal, Bioresour. Technol. 95 (2004) 255–257.
[5] M. Wang, Z.H. Huang, G.J. Liu, F.Y. Kang, Adsorption of dimethyl sulfide from aqueous solution by a cost-effective bamboo charcoal, J. Hazard. Mater. 190 (2011) 1009–1015.
[6] A.A. Ahmad, B.H. Hameed, Effect of preparation conditions of activated carbon from bamboo waste for real textile wastewater, J. Hazard. Mater. 173 (2010) 487–493.
[7] D. Fu, Y.H. Zhang, F.Z. Lv, P.K. Chu, J.W. Shang, Removal of organic materials from TNT red water by bamboo charcoal adsorption, Chem. Eng. J. 193–194 (2012) 39–49.
[8] S.Y. Wang, M.H. Tsai, S.F. Lo, M.J. Tsai, Effects of manufacturing conditions on the adsorption capacity of heavy metal ions by Makino bamboo charcoal, Bioresour. Technol. 99 (2008) 7027–7033.
[9] F.Y. Wang, H. Wang, J.W. Ma, Adsorption of cadmium (II) ions from aqueous solution by a new low-cost adsorbent—Bamboo charcoal, J. Hazard. Mater. 177 (2010) 300–306.
[10] Z.Q. Tan, J. Xiang, S. Su, H.C. Zeng, C.S. Zhou, L.S. Sun, S. Hu, J.R. Qiu, Enhanced capture of elemental mercury by bamboo-based sorbents, J. Hazard. Mater. 239–240 (2012) 160–166.
[11] X.J. Wang, Z. Wu, Y. Wang, W. Wang, X. Wang, Y.J. Bu, J.F. Zhao, Adsorption–photodegradation of humic acid in water by using ZnO coupled TiO_2/bamboo charcoal under visible light irradiation, J. Hazard. Mater. 262 (2013) 16–24.
[12] Y.X. Yang, K. Chiang, N. Burke, Porous carbon-supported catalysts for energy and environmental applications: A short review, Catal. Today 178 (2011) 197–205.
[13] K. Laohhasurayotin, S. Pookboonmee, Multifunctional properties of Ag/TiO_2/bamboo charcoal composites: Preparation and examination through several characterization methods, Appl. Surf. Sci. 282 (2013) 236–244.
[14] F.C. Yang, K.H. Wu, M.J. Liu, W.P. Lin, M.K. Hu, Evaluation of the antibacterial efficacy of bamboo charcoal/silver biological protective material, Mater. Chem. Phys. 113 (2009) 474–479.
[15] X.M. Zou, Y. Feng, C.M. Sheng, J. Liu, L.J. Lu, C. Hu, X.F. Huang, Novel application of bamboo-based fibers in a biological contact oxidation process, Water Sci. Technol. 69 (2014) 1534–1540.
[16] M. Zhang, B. Gao, S. Varnoosfaderon, A. Hebard, Y. Yao, M. Inyang, Preparation and characterization of a novel magnetic biochar for arsenic removal, Bioresour. Technol. 130 (2012) 457–462.
[17] X.J. Wang, Y. Wang, X. Wang, M. Liu, S.Q. Xia, D.Q. Yin, Y.L. Zhang, J.F. Zhao, Microwave-assisted preparation of bamboo charcoal-based iron-containing adsorbents for Cr(VI) removal, Chem. Eng. J. 174 (2011) 326–332.
[18] R.S. Zhao, Y.L. Liu, X.F. Chen, J.P. Yuan, A.Y. Bai, J.B. Zhou, Preconcentration and determination of polybrominated diphenyl ethers in environmental water samples by solid-phase microextraction with Fe_3O_4-coated bamboo charcoal fibers prior to gas chromatography–mass spectrometry, Anal. Chim. Acta 769 (2013) 65–71.
[19] P. Hu, Y.H. Zhang, F.Z. Lv, X.K. Wang, F.F. Wei, X.H. Meng, S.B. Jiang, Organic pollution removal from TNT red water using Cu-impregnated activated coke, Water Air Soil Pollut. 225 (2014) 1936–1945.
[20] A. Espíndola-Gonzalez, A.L. Martínez-Hernández, C. Angeles-Chávez, V.M. Castaño, C. Velasco-Santos, Novel crystalline SiO_2 nanoparticles via annelids bioprocessing of agro-industrial wastes, Nanoscale Res. Lett. 5 (2010) 1408–1417.
[21] C.T. Cherian, J. Sundaramurthy, M. Kalaivani, P. Ragupathy, P. Kumar, V. Thavasi, M.V. Reddy, C.H. Sow, S.G. Mhaisalkar, S. Ramakrishna, B.V.R. Chowdari, Electrospun α-Fe_2O_3 nanorods as a stable, high capacity anode material for Li-ion batteries, J. Mater. Chem. 22 (2012) 12198–12204.
[22] F.Z. Lv, L.L. Fu, E.P. Giannelis, G.G. Qi, Preparation of γ-Fe_2O_3/SiO_2-capsule composites capable of using as drug delivery and magnetic targeting system from

hydrophobic iron acetylacetonate and hydrophilic SiO_2-capsule, Solid State Sci. 34 (2014) 49–55.
[23] F. He, K. Lam, D. Ma, J. Fan, L.H. Chan, L.M. Zhang, Fabrication of graphene nanosheet (GNS)–Fe_3O_4 hybrids and GNS–Fe_3O_4/syndiotactic polystyrene composites with high dielectric permittivity, Carbon 58 (2013) 175–184.
[24] F.S. Bayburtskiy, Y.V. Baldokhin, M.R. Kisselev, H.U. Lubman, A.L. Petelin, T.V. Tsyganova, Preparation of a magnetic composite material with a set properties on the basis of the activated cargon and iron oxide, Oxid. Commun. 31 (2008) 942–953.
[25] G. Sharma, P. Jeevanandam, Single step thermal decomposition approach to prepare supported γ-Fe_2O_3 nanoparticles, Appl. Surf. Sci. 258 (2012) 3679–3688.
[26] J.D. Xiao, L.G. Qiu, X. Jiang, Y.J. Zhu, S. Ye, X. Jiang, Magnetic porous carbons with high adsorption capacity synthesized by a microwave-enhanced high temperature ionothermal method from a Fe-based metal-organic framework, Carbon 59 (2013) 372–382.